





successfully in the nano- science and nanotechnology research to provide researchers with an intuitive way to interact with materials and devices at the nanoscale. Guthold [24] tried to provide a virtual-environment interface to SPMs, giving a virtual tele-presence on the surface but downscaled by a factor of about a million to one.

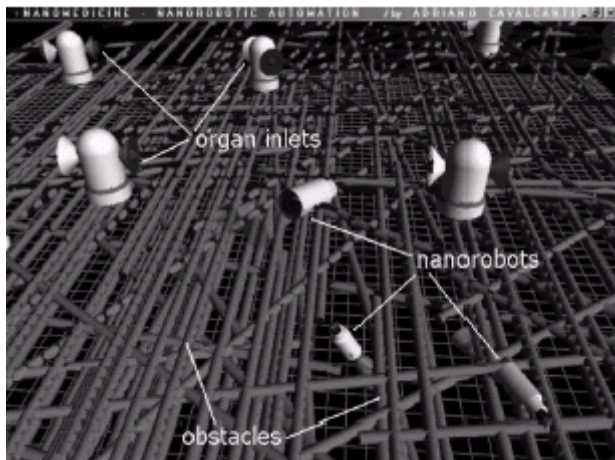


Figure 1: Virtual Environment, Top Camera View

The introduction of direct human–SPM interaction creates not only enhanced measurement capability (for instance, special transducers can provide a sense of touch to the nanomanipulator), but also presages a more fully automated technology that will enable nanofabrication and/or repair of nanostructures. A 3-D bionanomanipulation system integrated with a real-time virtual reality simulator has been proposed [21]. Nanoscale object manipulation systems have been applied with the use of computer graphics for teleoperation, where the requirements for such systems have been clearly established.

Virtual reality was considered a suitable approach for nanorobot design and for the use of macro- and microrobotics concepts given certain theoretical and practical aspects that focus on its domain of application.

The nanodevice design must be robust enough to operate in an aqueous environment with movement having six degrees of freedom (see Fig. 1). The virtual environment in our study is inhabited by nanorobots, biomolecules, obstacles, and organ inlets. Each nanorobot measures 650 nm in length and 160 nm in diameter. The biomolecule has a diameter of 10 nm and each obstacle has a diameter of 120 nm. The organ inlets are 400 nm in height and width with inlet orifices 720 nm in diameter. The trajectories and positions of each molecule which must be captured and assembled were generated randomly, and each one also has a probabilistic velocity and acceleration.

In the simulation, while some molecules have been captured (Fig. 2) other molecules are manipulated and assembled internally by the robot arm inside the proposed nanorobot. The nanorobot design is derived from biological models and is comprised of components such as *molecularsorting rotors* and a robot arm (*telescoping manipulator*) [13], [20]. The nanorobot exteriors considered in our design assumes a dandelion-like material to which may be attached an artificial

glycocalyx surface that minimizes fibrinogen (and other blood protein) adsorption and bioactivity, thus ensuring sufficient biocompatibility for the nanorobot to avoid immune system attack [18].

Different molecule types are distinguished by a series of chemotactic sensors whose binding sites have a different affinity for each kind of molecule [20].

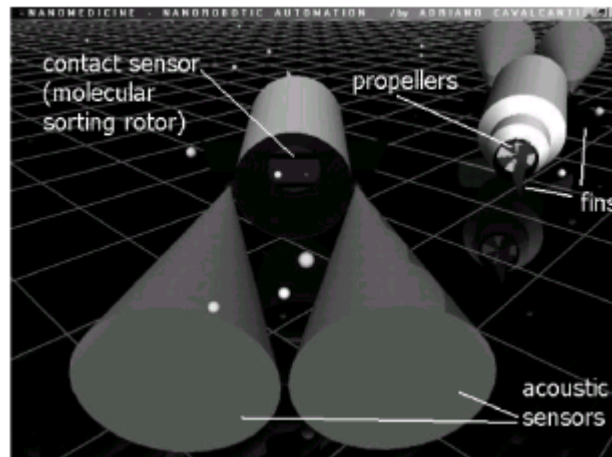


Figure 2: Molecular identification

Some concepts provided from underwater robotics were assumed for nanorobot locomotion. The nanorobot kinematic response can be predicted using state equations, positional constraints, inverse kinematics, and dynamics, while some individual directional component performance can be simulated using control system models of transient and steady-state response [6]. Plane surfaces (three fins total) and bidirectional propellers provide navigation, while two simultaneously counter rotating screw drives provide the propulsion [20]. The nanorobot lives in a world of viscosity, where friction, adhesion, and viscous forces are paramount and the gravitational force here is relatively negligible [13], [20]. In this world, a very low Reynolds number ( $Re$ ) is assumed for the kinetic calculations, where the fluid mechanics in small structures can usually be described by the classical continuum equations [13]. The ratio of inertial to viscous forces is determined by as expressed in (1)

$$Re = \frac{\rho V L}{\eta} \quad (1)$$

where  $\rho$  is the absolute viscosity of the fluid,  $V$  is the velocity,  $L$  is the fluid density, and  $\eta$  is a characteristic dimension.  $Re$  indicates whether the flow will be laminar or turbulent around an object of a given shape at a given flow velocity. For nanoscale dimensions in fluids of ordinary viscosities and velocities,  $Re$  is low and the flow is laminar [20]. The inertial force on the object is of order  $\rho V^2 L^3$  and the viscous drag force is of order  $6\pi\eta V L$ . In order to keep moving forward, a nanorobot of size  $m$  and velocity  $v$  must apply (femtonewtons,) and a much larger of motive force [20]. For instance, if motive power to a swimming nanorobot with radius  $m$ , and velocity  $cm/s$ , is suddenly stopped, then the nanorobot will “coast” to a halt in a time given by (2)

$$t_{\text{coast}} = \frac{\rho R_{\text{nanorobot}}^2}{15\eta} = 0.1 \quad (2)$$

where 0.1 is expressed in microseconds, and in a distance nm [4].

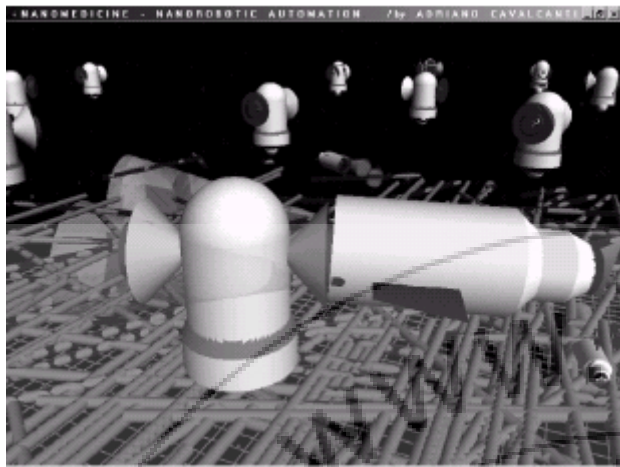


Figure 3: Nanorobot Molecule Delivery

Similarly with as the rotational frequency, if the nanorobot is rotating at a frequency Hz when its rotational power source is suddenly turned off, decays exponentially to zero in a time  $s$  and stops after turning through an angle, as expressed by (3)

$$\theta_{\text{total}} = \frac{2\pi f \tau R_{\text{rotor}}}{15\pi} \quad (3)$$

(3) or 40 rad in this instance [20]. The nanorobots use a macrotransponder navigational system for the main aspects of the nanorobot positioning, which allow high positional accuracy in each nanorobot's orientation [20]. Such a system might involve externally generated signals from beacons placed at fixed positions outside the skin [20]. Thus, the delivery positions that represent organ inlets requiring proteins to be injected are located in well-known locations for the nanorobot. If these organ inlets are or are not scheduled for injection at time, they change the team  $A$  (blue nanorobots) and team  $B$  (yellow nanorobots) delivery orifice colors in the simulation, opening or closing the orifice (Fig. 3). This better enables visualization of the organ inlets in which the agents are performing their delivery in the current time step of the simulation. The assembled molecules are thus delivered to specific locations by nanorobots docking at 2-  $m$  ( 1.4-  $m$  ) sites embedded at appropriate spatial intervals across the organ inlets' orifice [19], which is open for the delivery. The assembled molecule can be pumped by the molecular sorting rotors in 10 s [19].

The use of local perception should in most cases be quite sufficient for the overall set of tasks that our nanorobots are designed to perform. An explicit communication between each nanorobot partner sending the signal is required when a delivery is completed for the determined organ inlet, whereupon nanorobot  $B$  awaits a message from nanorobot  $A$  confirming that  $A$  has finished the delivery to the given organ inlet. Acoustic communication sensors [20] mounted within the nanorobot hull permit the nanorobot to communicate with its partner whether or not the organ inlet has received the required substance.

By using the nanorobot's local perception as much as possible and by sending the fewest possible messages to other nanorobots, unnecessary communication between the agents is reduced, thus minimizing energy consumption by the nanorobots.

Nanorobots satisfy their energy requirements via the chemical combination of oxygen and glucose [20], both of which are plentiful in the human body. The nanorobot includes external sensors to inform it of collisions and to identify when it has encountered an obstacle which will require a new trajectory planning. Aspects of the nonstructured opaque surrounding workspace, like the interior of the human body where the nanorobot is acting, must be considered in the navigational sensing design.

In robotics fields, there are often many kind of sensors, such as infrared, computer vision, chemical sensors, and so forth, which are normally used for robotics navigational purposes. Optical sensors have been widely applied in terrestrial mobile robotics, but these have an extremely limited range in a liquid environment. Types of sensors such as laser rangefinders [6] could be also used for underwater robotics but not for nanorobotics sensing because, for instance, the laser energy might excite or chemically alter the surrounding biomolecules that the nanorobot is trying to capture. Although the infrared sensor seems preferable for macroscale terrestrial robots, for underwater robots the most common sensor approach involves the use of sonar systems. Similarly, the most addressable approach for nanorobots in nanomedicine is to use acoustic waves [20]. The blue cones shown in Fig. 2 represent regions that the robot's sonar can "hear." Scientific visualization techniques permit rapid and precise geometric analysis to simulate a sonar classification system [6].

We used physically based simulation [3] to consider kinematics and frictional aspects specifically required for rigid body motion with hydrodynamics at low  $Re$  number for molecular assembly manipulation.

#### 4.2 Evolutionary Decision

We intend to construct and demonstrate the applicability of multirobot teams in timely sequenced work for capture, assembly, transport, and delivery of biomolecular pieces to a predefined set of organ inlets.

The use of multirobot teams to work cooperatively to achieve a single global task applied to nanotechnology is a field of research that is relatively new [9]. Research on collective robotics suggests that we should consider emulating the methods of the social insects to build decentralized and distributed systems that are capable of accomplishing tasks through the interaction of agents with the same structures and preprogrammed actions and goals. Thus, a careful decomposition of the main problem task into subtasks with action based on local sensor-based perception could generate multirobot coherent behaviors [33].

The approach for the nanomedicine problem here could be described as two multirobot teams which must cooperate



interactively to feed a set of organ inlets in the virtual environment under study. The importance of cooperative teamwork has led us to choose a high-level decision control model with adaptive evolutionary characteristics. Note that the proposed nanorobot model here includes no kind of nanorobot self replicating behavior [12]. Instead, our model uses an evolutionary approach strictly for the combinatorial analyses, allowing the nanorobots to react cooperatively in an uncertain environment with a well defined preprogrammed set of actions. The model used here, often cited in the literature as

Genetic Algorithms (GA), relies on concepts derived from evolution and genetics [8]. Each solution here is described as a chromosome regarding the nanorobot decision on how, when, and what organ inlets to attend in the dynamic scenery. Each decision required to be taken by the nanorobot always follows the programmed set of actions rigidly pre-established in our design by the fitness/ objective function. Equation (4) represents our fitness function, where the nanorobots maximize the protein levels for the selected organ inlets. The variable induces the nanorobot to catch a number of molecules as closely as possible to the desired delivery mean, while brings the nutritional levels as close as possible to

inlets to be attended by the nanorobots at each time step of the simulation.

Each pair is comprised of nanorobots from team A, and B. The organ inlets selected to be fed at time have to be fed first by the agent A, then by B, and so forth. Both agents must take care to avoid applying an overdose or deficiency of the injected substances.

Table 1

$r, t, \bar{i}$	subscript denoting: robot, time, organ inlet;
$w_{\bar{i}}^t$	organ inlets' desirable nutritional target level;
$y^t$	surplus/deficit to the desired assembled mean;
$z$	keep the nutritional levels close to the target;
max, min	upper and lower bound parameter;
$A, B$	respective robotics teams;
$n$	size of time in the simulated scenery;
$m$	total of organ inlets to be fed;
$L$	robot load capacity;
$x_{\bar{i}}^t$	substance amount injected in the organ inlet $\bar{i}$ ;
$Q^t$	total assembled molecule by $r$ in $t$ ;
$w_{\bar{i}}^t$	chemical state of the organ inlet $\bar{i}$ at time $t$ ;
$s_{\bar{i}}^t$	nutrients consumption by the organ inlet $\bar{i}$ ;
$d$	desired assembled substances rate;
$\gamma$	parameter to look ahead at nutritional levels;
$\mu_{\bar{i}}^t$	Boolean variable;
$\Omega$	determines if $r$ belongs to team A or B;
$\Delta$	maximum to be injected at organ $\bar{i}$ in $t$ .

$$\max f(r_{\Omega}) = \sum_{t=1}^n \sum_{\bar{i}=1}^m w_{\bar{i}}^t - |y^t| - |z^t| \quad (4)$$

$$\text{s.t. } z_{\bar{i}}^t = w_{\bar{i}}^{t+1} - w_{\bar{i}}^t \quad (5)$$

$$y^t = Q^t - d \quad (6)$$

$$Q^t = \sum x_{\bar{i}}^t \leq L \quad (7)$$

$$x_{\bar{i}}^t = \mu_{\bar{i}}^t x_{\bar{i}}^{\text{max}} \quad (8)$$

$$\mu_{\bar{i}}^t \leq \Delta_{\bar{i}}^{\text{max}} \quad (9)$$

$$w_{\bar{i}}^{t+1} = w_{\bar{i}}^t - \gamma s_{\bar{i}}^t + x_{\bar{i}}^t \quad (10)$$

$$w_{\bar{i}}^{\text{min}} \leq w_{\bar{i}}^t \leq w_{\bar{i}}^{\text{max}} \quad (11)$$

$$\mu_{\bar{i}}^t \in \{[0, 100] \vee [0, 1]\} \quad (12)$$

$$\Omega \in \{A, B\} \quad (13)$$

The multirobot team behavior interaction rule is described in Table I, with, denoting if the robot belongs to team A or B; is the minimum defined to be captured by each robot at time step, where,, and represent the kind of molecule to be assembled by ; therefore

$$\beta \begin{cases} \Omega = A \Rightarrow \beta = e \\ \Omega = B \Rightarrow \beta = l_e \end{cases} \quad (14)$$

$$\delta = y. \quad (15)$$

$r, t, \bar{i}$	subscript denoting: robot, time, organ inlet;
$w_{\bar{i}}^t$	organ inlets' desirable nutritional target level;
$y^t$	surplus/deficit to the desired assembled mean;
$z$	keep the nutritional levels close to the target;
max, min	upper and lower bound parameter;
$A, B$	respective robotics teams;
$n$	size of time in the simulated scenery;
$m$	total of organ inlets to be fed;
$L$	robot load capacity;
$x_{\bar{i}}^t$	substance amount injected in the organ inlet $\bar{i}$ ;
$Q^t$	total assembled molecule by $r$ in $t$ ;
$w_{\bar{i}}^t$	chemical state of the organ inlet $\bar{i}$ at time $t$ ;
$s_{\bar{i}}^t$	nutrients consumption by the organ inlet $\bar{i}$ ;
$d$	desired assembled substances rate;
$\gamma$	parameter to look ahead at nutritional levels;
$\mu_{\bar{i}}^t$	Boolean variable;
$\Omega$	determines if $r$ belongs to team A or B;
$\Delta$	maximum to be injected at organ $\bar{i}$ in $t$ .

We used real time and parallel processing techniques, where both teams react adaptively to any stimulus produced by their partners' decisions, with the model visualization in real time. The study of smart multirobot behavior in a single global environment enables concepts related to the use of local perception for reactive agents [5], [33]. Multidisciplinary control design addresses the nanorobot's multimodular system architecture [10]. A feed forward neural networks model discussed below was used for the nanorobot motion control, wherein each nanorobot visits in a shorter time the organ inlets that were pre-attributed to that nanorobot in order to gather information for the next time step decision from the 3-D workspace.

### 4.3 Neural Motion

A connectionist model using artificial neural networks was chosen for the motion control and shortest-path problem solution, beginning with a dynamic combinatorial problem for each time step simulation. The classical problem of finding an optimal three-dimensional shortest path avoiding 3-D polygonal obstacles is typically NP-hard [3]. The use of a nondeterministic approach to solve the motion control seems to be the appropriate technique in such cases [23]. We

We have decomposed the total set of organ inlets, assigning for each pair of nanorobots a specified number of organ

have implemented a feed forward or acyclic network due to its suitability for probabilistic calculations. The particular model implemented here is a stochastic feed forward neural network [28], which requires a lower computational effort in comparison with a back propagation algorithm [25] and a better performance in comparison with a *greedy* heuristic approach [59]. The features of the algorithm for the implemented neural network could be represented by (16)

$$p_{ij}(X_j) \subseteq \{X_1, X_2, \dots, X_{j-1}\} \quad (16)$$

where represents a vector, consisting of the two-valued random variables, defining a topology composed of stochastic neurons. With representing the range of hidden layers, which leads the network to be optimized at the time step, it represents each destiny to be achieved for throughout the simulation. The units in the network are organized into a 2-D matrix, with rows by columns, where and are the costs matrix of destinations for each evolutionary agent, which tries to complete its set of tasks successfully as fast as possible. Let the output of the unit in row and column be, where. This means that the referred destination is visited at the  $t$ th stop, with otherwise. Therefore, a solution cost for each agent routing could be expressed by (17)

$$\min C_r^k = \sum_{i=1}^{m_i} \sum_{j=1}^{n_i} v_{ij}^k u_{ij}^k. \quad (17)$$

Once having obtained both routes (route on and route off), which are composed respectively of the organ inlets to be supplied and the organ inlet whose nutritional level is to be verified, then the nanorobot performs the trajectory visiting the subset of organ inlets assigned to it, first executing the whole delivery route, and afterwards beginning the verification route. One positive aspect of a feed forward neural network is that it requires low computational effort to achieve motion control in a workspace with six degrees of freedom [25]. We use binary cues to trigger the behavioral response as a common mechanism for action and for governing different phases of activity in tasks—as is done by social insects [11]. In this manner, activation of a motor behavior is not dependent on a specific perceptual cue, but rather on the decision that results from sensor processing. The advantage is that the design of the motor behavior does not change when different sensor types or alternate feature extraction techniques are used, since the information needed by the motor behavior is the same binary vector in both cases [33].

## 5. Simulation and Conclusion

Biomolecular machine system designs that are capable of accomplishing successfully a set of preprogrammed tasks in a 3-D workspace is a new challenge for control investigation. We describe the study of an automation model and the respective visualization tools to follow up the analyses for the control theory development based on experimental results. Nanorobots' monitoring nutrient concentrations in a 3-D workspace is a possible application of nanorobots in medicine, among other biomedical problems [20]. One interesting nanorobot application is to assist inflammatory cells (or white cells) leaving blood

vessels to repair injured tissues [7]. Also the nanorobot could be used to process specific chemical reactions in the human body as ancillary devices for injured organs. Nanorobots equipped with nanosensors could be developed to detect glucose demand in diabetes patients [30]. Nanorobots could also be applied in chemotherapy to combat cancer through superior chemical dosage administration and a similar approach could be taken to enable nanorobots to deliver anti-HIV drugs. Such drug-delivery nanorobots have been termed "pharmacytes" by Freitas [20].

The neural motion control was successfully used with real-time response for the circumstance where the nanorobots must capture molecules and visit a predefined set of delivery points, avoiding random obstacles and collision with other mobile nanorobots, and trying at the same time to minimize the time required.

These tasks were satisfactorily accomplished using the neural networks approach, wherein the nanorobots calculated their complete trajectories with a cost minimization of 37% in the required distance good improvement in comparison with a *greedy* solution for the motion control optimization. Realizing revolutionary applications of nanorobots to health or environmental problems raises new control challenges.

The design and the development of complex nanosystems with high performance should be addressed via simulation to help pave the way for future medical nanorobotic systems.

## References

- [1] L. M. Adleman. (1995) On constructing a molecular computer. *DNA Based Computers* [Online]. Available: <http://olymp.wu-wien.ac.at/usr/ai/frisch/local.html>
- [2] G. D. Bachand and C. D. Montemagno, "Constructing organic/inorganic NEMS devices powered by biomolecular motors," *Biomed. Microdev.*, vol. 2, pp. 179–184, 2000.
- [3] D. Baraff, "Dynamic simulation of non-penetrating rigid bodies," PhD Thesis, Dept. Comput. Sci., Cornell Univ., Ithaca, NY, 1992.
- [4] H. C. Berg, "Dynamic properties of bacterial flagellar motors," *Nature*, vol. 249, May 1974.
- [5] H. Bojinov, A. Casal, and T. Hogg, "Multiagent control of self-reconfigurable robots," in *Proc. IEEE ICMAS Int. Conf. Multiagent Systems*, 2000, pp. 441–455.
- [6] D. P. Brutzman, Y. Kanayama, and M. J. Zyda, "Integrated simulation for rapid development of autonomous underwater vehicles," in *IEEE Autonomous Underwater Vehicle Conf.*, Washington DC, Jun. 1992, pp. 3–10.
- [7] A. Casal, T. Hogg, and A. Cavalcanti, "Nanorobots as cellular assistants in inflammatory responses," presented at the IEEE BCATS Biomedical Computation at Stanford 2003 Symp., Stanford, CA, 2003.
- [8] A. Cavalcanti, "Assembly automation with evolutionary nanorobots and sensor-based control

- applied to nanomedicine,” *IEEE Trans. Nanotechnol.*, vol. 2, no. 2, pp. 82–87, Jun. 2003.
- [9] A. Cavalcanti and R. A. Freitas, Jr., “Autonomous multi-robot sensor-based cooperation for nanomedicine,” *Int. J. Nonlinear Sci. Numer. Simul.*, vol. 3, no. 4, pp. 743–746, Aug. 2002.
- [10] W. Chen and K. Lewis, “A robust design approach for achieving flexibility in multidisciplinary design,” *AIAA J.*, vol. 37, no. 8, pp. 982–990, 1999.
- [11] H. A. Downing and R. L. Jeanne, “Nest construction by the paperwasp, *Plistes*: a test of stigmergy theory,” *Animal Behav.*, vol. 36, pp. 1729–1739, 1988.
- [12] K. E. Drexler, D. Forrest, R. A. Freitas, Jr., J. S. Hall, N. Jacobstein, T. McKendree, R. Merkle, and C. Peterson. (2001) A Debate About Assemblers. *Inst. Mol. Manuf.* [Online]. Available: <http://www.imm.org/SciAmDebate2/whitesides.html>
- [13] K. E. Drexler, *Nanosystems: Molecular Machinery, Manufacturing, and Computation*. New York: Wiley, 1992.
- [14] G. Fishbine, *The Investor’s Guide to Nanotechnology and Micromachines*. New York: Wiley, 2001.
- [15] R. A. Freitas, Jr., “Progress in nanomedicine and medical nanorobotics,” in *Handbook of Theoretical and Computational Nanotechnology*, M. Rieth and W. Schommers, Eds. Stevenson Ranch, CA: American Scientific, 2005, to be published.
- [16] “Current status of nanomedicine and medical nanorobotics,” *J. Comput. Theor. Nanosci.*, vol. 2, 2005, to be published.
- [17] R. A. Freitas, Jr. and R. C. Merkle, *Kinematic Self-Replicating Machines*. Georgetown, TX: Landes Biosci., 2004.
- [18] R. A. Freitas, Jr., *Nanomedicine*. Georgetown, TX: Landes Biosci., 2003, vol. 2A, Biocompatibility.
- [19] R. A. Freitas, Jr. and C. J. Phoenix. (2002) Vasculoid: a personal nanomedical appliance to replace human blood. *J. Evol. Technol.*
- [20] R. A. Freitas, Jr., *Nanomedicine*. Georgetown, TX: Landes Biosci., 1999, vol. 1, Basic Capabilities.
- [21] T. Fukuda and T. Arai, “Prototyping design and automation of micro/nano manipulation system,” in *Proc. IEEE Int. Conf. Robotics and Automation (ICRA ’00)*, vol. 1, pp. 192–197.
- [22] L. Geppert, “The amazing vanishing transistor act,” *IEEE Spectr.*, vol. 30, no. 10, pp. 28–33, Oct. 2002.
- [23] R. Grzeszczuk, D. Terzopoulos, and G. Hinton, “NeuroAnimator: fast neural network emulation and control of physics-based models,” in *Proc. ACM SIGGRAPH ’98 Conf.*, M. Cohen, Ed., pp. 142–148.
- [24] M. Guthold, “Controlled manipulation of molecular samples with the nano-manipulator,” *IEEE/ASME Trans. Mechatron.*, vol. 5, no. 2, pp. 189–198, 2000.
- [25] M. T. Hagan, H. B. Demuth, and O. D. Jesús, “An introduction to the use of neural networks in control systems,” *Int. J. Robust Nonlinear Control*, vol. 12, no. 11, pp. 959–985, Sep. 2002. 140 IEEE TRANSACTIONS ON NANOBIOSCIENCE, VOL. 4, NO. 2, JUNE 2005
- [26] M. Hagiya, “From molecular computing to molecular programming,” in *Proc. 6th DIMACS Workshop DNA Based Computers*, 2000, pp. 198–204.
- [27] K. Hamad-Schifferli, J. J. Schwartz, A. T. Santos, S. Zhang, and J. M. Jacobson, “Remote electronic control of DNA hybridization through inductive coupling to an attached metal nanocrystal antenna,” *Nature*, vol. 415, pp. 152–156, Jan. 10, 2002.
- [28] S. Haykin, *Neural Networks a Comprehensive Foundation*, 2<sup>nd</sup> ed. Englewood Cliffs, NJ: Prentice-Hall, 1999.
- [29] A. Hellemans, “German team creates newtype of transistor-like device,” *IEEE Spectr.*, vol. 40, no. 1, pp. 20–21, Jan. 2003.
- [30] E. Katz, A. Riklin, V. Heleg-Shabtai, I. Willner, and A. F. Bückmann, “Glucose oxidase electrodes via reconstitution of the apo-enzyme: tailoring of novel glucose biosensors,” *Anal. Chim. Acta.*, vol. 385, pp. 45–58, 1999.
- [31] M. Khatib, B. Bouilly, T. Simeon, and R. Chatila, “Indoor navigation with uncertainty using sensor based motions,” in *Proc. 1997 IEEE Int. Conf. Robotics and Automation*, pp. 3379–3384.
- [32] J.-W. Kim, A. Malshe, and S. Tung, “Bio-inspired MEMS: a novel microfluidics system actuated by biological cell motors,” presented at the 2003 Institute of Biological Engineering (IBE) Annu. Meeting, Athens, GA.
- [33] C. R. Kube and H. Zhang, “Task modeling in collective robotics,” *Auton. Robots*, vol. 4, no. 1, pp. 53–72, 1997.